Evaluation of True Polarization Diversity for MIMO Systems

Juan F. Valenzuela-Valdés, Miguel A. García-Fernández, Antonio M. Martínez-González, and David A. Sánchez-Hernández, *Senior Member, IEEE*

***Abstract*—MIMO systems where multipath fading is only partially correlated could use polarization diversity to provide a higher diversity gain. Recent letters have proposed the use of tri-polarized antennas and a novel true polarization diversity (TPD) scheme. In this paper, the full potential of TPD is evaluated with both simulations and measurements and compared to conventional orthogonal polarization diversity (OPD). MIMO system performance with respect to capacity and diversity gain is obtained through the use of multimode-stirred chambers for both isotropic and non-isotropic environments. Simulated and measured results in over 591 different MIMO systems show that TPD outperforms conventional OPD for reduced volumes. Likewise, it has been demonstrated that TPD can be effectively combined with spatial diversity to nearly double the diversity gain and MIMO capacity for the same available handset volume.**

***Index Terms*—Diversity methods, MIMO systems, polarization, reverberation chamber, spatial correlation.**

I. Introduction

RECENT years have witnessed an increasing interest in MIMO systems. Capacity is expected to increase linearly with the number of employed antennas for rich multipath environments [1]. Yet, the high simulated capacities of MIMO systems for both correlated and uncorrelated scenarios [1]–[3] have not been obtained with realistic channels [4]. When in environments dominated by line of sight (LoS) conditions (Ricean-like), a linear increase in capacity will require either a higher spatial distance between antennas or additional polarization states [5]. In fact, for base stations and spatial diversity only, at least 20λ horizontal and between 11 and 13λ vertical separation distances are required for efficient spatial outdoor diversity in practice [6]–[8]. In base stations, however, the angular field of view is limited and high above the scatters. This implies a small arrival angle spread, which is not the case for communication devices down in the scattering medium. Hence, the required spatial separation at the mobile station depends on the effective scattering radius of the area in which the mobile is located. Despite this advantage, other ways of de-correlating MIMO branches are desired in handset MIMO due to the inherent volume limitation. Consequently, polarization diversity has recently gained attention. The improvement granted by polarization diversity in wireless systems is typically obtained by an additional de-correlated channel provided by a polarization state made orthogonal to the existing one. A randomly oriented linearly-polarized antenna is also typically used at the receiver for evaluating polarization diversity. In this scheme the cross-polarization discrimination (XPD) factor is the usual evaluation parameter. Multiple scattering, however, may not be sufficient for a given polarization to decouple half its power into the orthogonal polarization [1]. Moreover, both reflection and diffraction processes are polarization sensitive. Channel behavior is therefore different for different polarization states [9]. This enhances the potential of using multiple polarization states to avoid the possible lack of richness in multipath. Recently, a tri-axial combination of polarization and pattern diversity has also been proposed [9], [10]. A recent letter [11] has proposed a novel true polarization diversity (TPD) technique. In [11] only preliminary diversity gain results for 3×3 MIMO systems were analyzed. Yet, the full potential of TPD for $m \times n$ MIMO systems where any polarization state could be employed is not fully addressed in the literature and requires more research. This is mainly due to the inherent complexity of the coupling mechanisms between different polarizations states [12]. In fact, an accurate prediction of the correlation coefficient between two dipoles separated by both a spatial distance and an arbitrary angular position has not been available until very recently [13].

In this paper diverse simulations and measurements using multimode-stirred chambers are performed to validate the potential of TPD for increasing diversity gain and MIMO capacity. TPD simulations in this paper make use of the formulation in [13]. Results demonstrate that TPD can be effectively combined with spatial diversity to nearly double the diversity gain and MIMO capacity for the same available volume. TPD outperforms conventional orthogonal polarization diversity (OPD) for reduced volumes, which is reported here for the first time. The paper is organized as follows. Section II describes the measurement technique and set-up. Section III validates the testing system through measurements. Section IV shows simulations and measurements of spatial, conventional OPD and TPD techniques, as well as combinations of these. Section V provides a discussion on the obtained results. Conclusions are outlined in Section VI.

Manuscript received May 26, 2008; revised May 30, 2009. First published July 07, 2009; current version published September 02, 2009. This work was supported in part by the Spanish National R&D Programme through TEC2008-05811.

J. F. Valenzuela-Valdés is with EMITE Ing, Edificio CEEIM, E-30100 Murcia, Spain (e-mail: juan.valenzuela@emite-ingenieria.es).

M. A. García-Fernández and A. M. Martínez-González are with the Departamento de Tecnologías de la Información y Comunicaciones, Universidad Politécnica de Cartagena, Cartagena E-30202, Spain.

D. A. Sánchez-Hernández is with the Departamento de Tecnologías de la Información y Comunicaciones, Universidad Politécnica de Cartagena, Cartagena E-30202, Spain (e-mail: david.sanchez@upct.es).

Color versions of one or more of the figures in this paper are available online at http://ieeexplore.ieee.org.

Digital Object Identifier 10.1109/TAP.2009.2027042

0018-926X/$26.00 © 2009 IEEE

II. Measurement Technique and Set-Ups

A. Multimode-Stirred Chambers

The instantaneous channel capacity for MIMO systems is well defined in [4], [14]–[17] by

$$C_{\mathrm{MIMO}} = \log_2\left(\det\left(I_R + \frac{SNR}{T} * H * H'\right)\right) \frac{\frac{\mathrm{bits}}{\mathrm{s}}}{\mathrm{Hz}} \quad (1)$$

where H is the measured channel transfer matrix and H' is the conjugate transpose of H. The system has T antennas at the transmitter and R antennas at the receiver, and I_R is the identity matrix with dimension R. In an independent identically distributed (i.i.d.) Rayleigh environment this capacity can be approximated for high signal-to-noise ratio (SNR) to [1], [2] $C \approx \min(T,R)\log_2(SNR)$ bits/s/Hz. This growth potential is extraordinary since for uncorrelated orthogonal channels each 3-dB increase in transmit SNR will result in roughly $\min(T,R)$ bit/s/Hz capacity increase in contrast to 1 bit/s/Hz capacity gain in single-antenna systems. In real multipath scenarios some correlation exists, which requires more research [1], [18].

Laboratory research can be performed over an artificially-generated multipath environment. This can be done with multimode-stirred chambers. A multimode-stirred chamber is a metal cavity or coupled-cavities sufficiently large to support many natural resonant modes (multimode). The excited modes are perturbed with stirrers and other apparatus in order to create the desired multipath. Multimode-stirred chambers have already demonstrated their ability to reproduce multipath propagation environments typically found in indoor and urban wireless environments [19], [22]. While avoiding cumbersome outdoor measurements, compact-size chambers provide accurate and reliable ways of validating measurements for MIMO systems and diversity schemes [23]. Recently, multimode-stirred chambers have been used to emulate non-isotropic environments [24], Ricean-fading environments [25], indoor environments with different rms delay spreads [26], wideband in-vehicle environments [27], keyhole effects [28] or metallic windows, trees, walls and other artefacts in buildings [29]. In consequence, the emulation performed in multimode-stirred chambers has abandoned the classic Clarke's model.

B. Measurement Technique

With the use of appropriate equipment several MIMO parameters can be evaluated through adequate processing of the measured scattering (S) parameters in a multimode-stirred chamber, particularly diversity gain and MIMO capacity [22], [23]. The S-parameters are gathered between the measured port and the transmitting antennas for all variable positions and for all frequency points, as illustrated in Fig. 1. This is a common approach used to determine the statistical behavior of a multimode-stirred chamber [30]. The statistics of the measured S-parameters are equivalent to the statistics of the field components [30]. This should be no surprise, since a measurement between two antennas is essentially a measurement of the transfer function of a given radio propagation

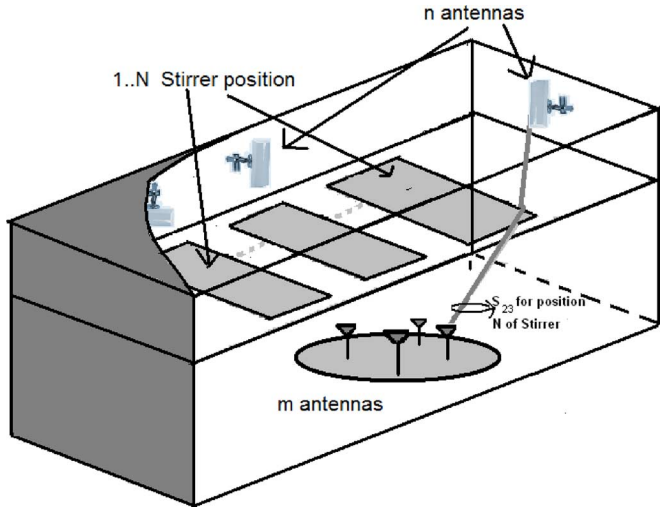

Fig. 1. The multipath environment emulated by a multimode-stirred chamber.

environment [31]. In our case, the measured S-parameters give the transfer function of the multimode-stirred chamber and hence the environment statistics. The innate repeatability of measurements in multimode-stirred chambers is an excellent feature for MIMO measurements. Measured S-parameters between the transmitting antennas (S_{mn}) and the MIMO array antennas (S_{nn}) are first averaged over stirred positions by [32],

$$\bar{S}_{mn} = \frac{1}{N}\sum_{\mathrm{stirred}} S_{mn} \quad and \quad \bar{S}_{nn} = \frac{1}{N}\sum_{\mathrm{stirred}} S_{nn} \quad (2)$$

where N is the total number of variable positions. At low frequencies it is also advantageous to perform stirring over a small frequency band. This is named frequency stirring, and it is performed to get more independent field samples representing a richer multipath environment. Changing the frequency changes the electrical size of the chamber, which has the effect of exciting different modes. Since some commercial systems like GSM use frequency hoping, this feature of multimode-stirred chambers emulates realistic environments. In some situations the S-parameters are normalized to obtain a better accuracy for the radiation efficiency as [33]

$$S'_{mn} = \frac{S_{mn}}{\sqrt{1-(\bar{S}_{mn})^2}\sqrt{1-(\bar{S}_{nn})^2}}. \quad (3)$$

The average net transfer function of the chamber becomes [23]

$$T = \frac{1}{N}\sum_{\mathrm{stirred}} |S'_{mn}|^2. \quad (4)$$

The processed S-parameters represent estimates of the channel matrix H of multipath communication channels set up between the transmitting antennas and the MIMO array inside the chamber. Diversity gain for the selection- or maximal ratio-combining techniques is obtained from the processed

S-parameters by evaluating the cumulative probability distributions of the measured channel samples received at each MIMO array antenna by [33]

$$h_{mn} = \frac{\left(S_{mn} \sqrt{e_{\mathrm{ref}} (1 - \left| \bar{S}_{nn} \right|^2)} \right)}{T_{\mathrm{ref}}} \tag{5}$$

where T_{ref} is the net chamber transfer function for a calibrated reference antenna with radiation efficiency e_{ref}. Channel capacity, the upper bound of the potential spectral efficiency, is calculated using the channel estimates h_{mn} in (5) between each of array elements and each one of the transmitting antennas. Thus, the $m \times n$ radio channels represent a $m \times n$ MIMO system, with n being the number of receiving antennas and m the number of transmitting antennas. With only one transmitting antenna the normalized channel estimates are obtained by [33]

$$H_{1\times n} = [h_{11} \quad h_{12} \quad \ldots \quad h_{1n}]. \tag{6}$$

For each channel matrix estimates $H_{m\times n}$, the channel capacity is calculated for a specific *SNR* range using the Frobenius matrix norm of the channel coefficient by

$$\|\mathrm{H}\|_F = \sqrt{\sum_{i=1}^{m} \sum_{j=1}^{n} |h_{i,j}|^2}. \tag{7}$$

In this way a graph of maximum average channel capacity estimates versus SNR is obtained. Similarly, other MIMO parameters such as the correlation coefficients can also be evaluated in the chamber.

C. Measurement Set-Ups

Measurements illustrated in this paper have been performed with the RC800 reverberation chamber for isotropic environments and the 8×8 MIMO Analyzer for non-isotropic environments, both in connection to the Rohde & Schwarz ZVRE Vector Network Analyzer (9 kHz to 4 GHz) and emulating Rayleigh-fading. The RC800 has dimensions of 0.8 m $\times$ 1 m $\times$ 1.6 m, 3 wall-mounted exciting antennas, polarization stirring due to different antenna exciting elements [35], 2 mechanical mode stirrers and 1 rotating platform. The MIMO Analyzer is a second generation multicavity multimode-stirred chamber with dimensions of 0.82 m $\times$ 1.275 m $\times$ 1.95 m, 8 exciting antennas, polarization stirring due aperture-coupling and to the different orientation of the antenna exciting elements, 3 mechanical and mode-coupling stirrers, 1 holder-stirrer and variable iris-coupling. The RC800 was set up for 25 platform stirring positions [34] with 15 different stirrer positions for each platform position and 100 MHz frequency stirring. In conventional multimode-stirred chambers like the RC800 the received signal becomes normally (Gaussian) distributed, with the associated magnitude following a Rayleigh distribution and the phase following a uniform distribution over 2π while the elevation distribution of the incoming waves is uniform. This allows for an emulation of multipath environments with Rayleigh-fading distribution of samples and isotropic scattering [19]. The MIMO Analyzer was set-up for 3 holder positions with 15 different mechanical stirrer positions for each holder position, 12 iris-coupling aperture stirring and 20 MHz frequency stirring. On top of the emulation capabilities of the RC800, the variable iris-coupling between multiple cavities of the MIMO Analyzer, in conjunction with an operating mode with an open door, make it capable of emulating both isotropic and non-isotropic fading environments for both Rayleigh and Rician distributions.

Each isolated antenna was measured in a different position within the chambers. This is also known as synthetic array measurements and is similar to the switched-array technique for MIMO measurements [36]. Less than 0.2% maximum capacity differences have been measured due to polarization imbalance. Measurements were performed at 900 MHz and commercial $\lambda/2$ 001-B-019 dipoles with operating ranges from 890 to 3000 MHz were used as the MIMO array antennas.

III. System Validation and Measurements

In order to validate measured results in a multimode-stirred chamber, the Rayleigh-fading spatial diversity results in [1] were replicated. Fig. 2 depicts the ergodic capacity of i.i.d. Rayleigh-fading 3×3 MIMO channels reproduced in the RC800 chamber with measured correlation coefficients of $\zeta = 0.1$, 0.5 and 0.8. In this figure results from [1] are also depicted for the same emulated scenarios. A good matching is observed in this figure between simulation and measurements, particularly at the SNR typically used for comparisons (15 dB) and for low correlation coefficients. This goodness of fit validates the proposed measurement set-up for emulating Rayleigh-fading scenarios with respect to capacity. Fig. 3(a) illustrates how the correlation coefficient ζ and the spatial diversity gain for 3×2 MIMO depend on the spatial separation $D(d/\lambda)$ through simulations [13] and measurements in the multimode-stirred chamber. Similarly, Fig. 3(b) illustrates how the correlation coefficient ζ and the TPD gain depend on the angular separation $d\theta(^\circ)$. It has been assumed for some time now that nearly full capacity is achieved for correlation coefficients ~ 0.5. A correlation coefficient ~ 0.5 is obtained with a spatial separation of $D = 0.21$. From Fig. 3 it is confirmed that in spatial diversity schemes a negligible diversity gain increase is obtained when using correlation coefficients ζ below ~ 0.5. This agrees well with previous works [1], [2],[17], [18]. It is also clear from this figure that TPD performs in a way similar to spatial diversity. In fact, TPD also shows a limit in angular separation values above which diversity gain increase is negligible. The limit was found to be $d\theta = 45^\circ$. For $d\theta = 45^\circ$ the measured correlation coefficient ζ is ~ 0.5, which is consistent with the results obtained for spatial diversity.

In real environments any polarization state can be received despite specific polarization states are used in transmission [38]. The chambers emulate well this polarization response of real channels by removing any polarization imbalance for both linearly polarized and circularly polarized antennas. This is done by using differently-polarized fixed antennas and averaging their transfer functions [35]. In consequence, TPD can be tested in the chambers. TPD employs arbitrary polarization

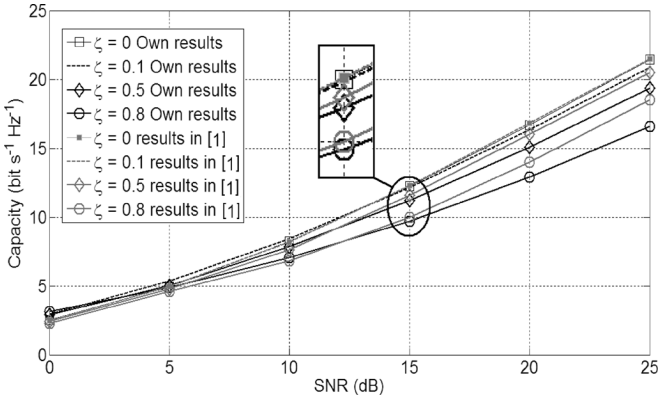

Fig. 2. Comparison of capacity (bits/s/Hz) versus SNR (dB) between [1] and RC800-measured results with correlation coefficient ζ as a parameter.

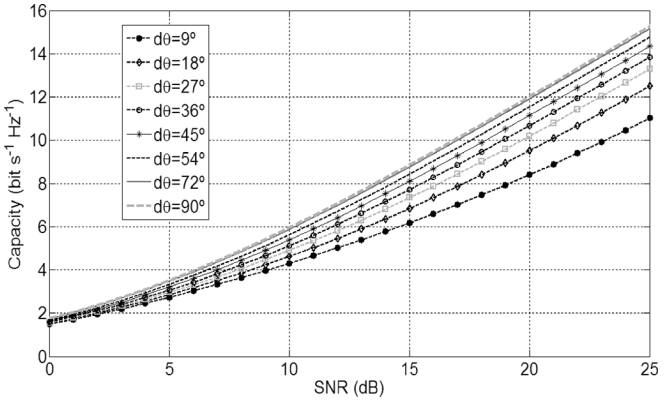

Fig. 4. 3×2 MIMO Capacity (bits/s/Hz) versus SNR (dB) with $\mathrm{D} = 0$ and angular separation $\mathrm{d}\theta$ between antennas as a parameter.

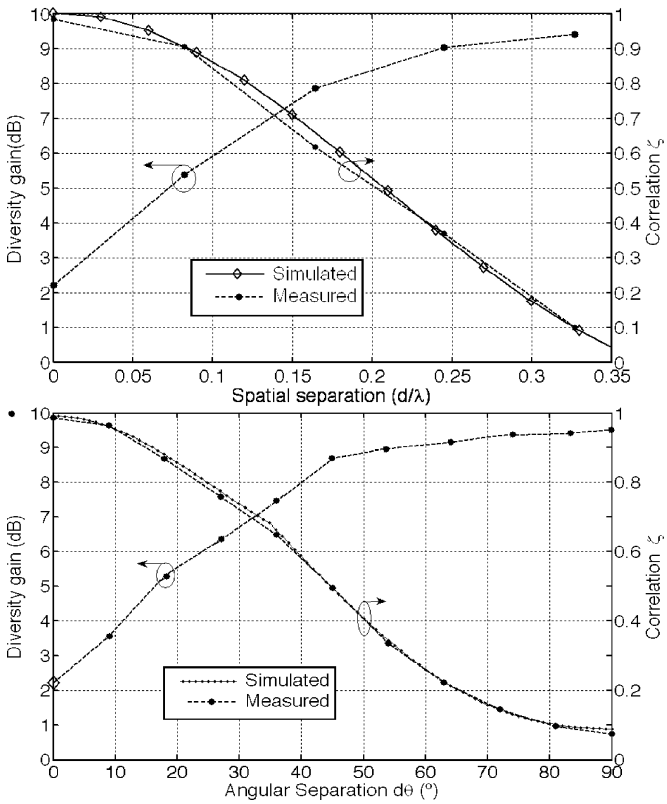

Fig. 3. 3×2 MIMO systems. A(Up): Correlation and spatial diversity gain versus wavelength-normalized spatial separation (d/λ). B(Down): Correlation and true-polarization diversity gain versus angular separation.

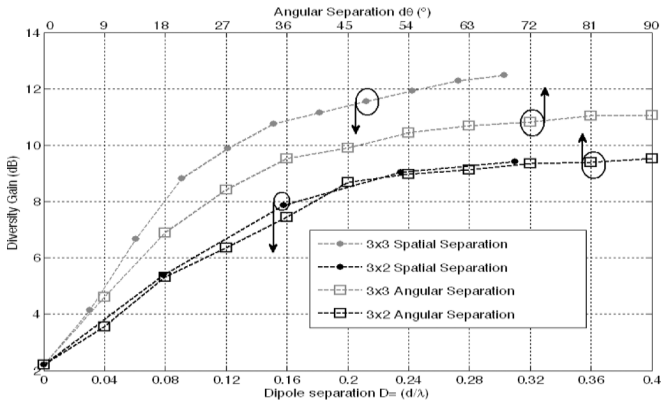

Fig. 5. Measured diversity gain versus wavelength-normalized spatial separation $D = (\mathrm{d}/\lambda)$ and angular separation $d\theta(^\circ)$ for 3×2 and 3×3 MIMO systems.

states with dipole inclination angles ranging from to 0 to $\alpha_{\max}$ and $\beta_{\max}$, where $\alpha_{\max}$ and $\beta_{\max}$ are the maximum allowable inclination angles respect to horizontal and vertical axes, respectively. In the tested MIMO arrays in this paper one-axis (1D) TPD ($\beta_{\max} = 0$) was used with sequential and non repeatable polarization states. The polarization state for the nth antenna element is then represented by a pair ϕ_n, θ_n given by

$$\phi_n = (n-1) * \frac{\alpha_{\max}}{N} \quad \text{and} \quad \theta_n = (n-1) * \frac{\beta_{\max}}{N} \qquad (8)$$

where N is the total number of receiving antennas. In this way an arbitrary angular separation between contiguous dipoles is employed in an equivalent way that an arbitrary spatial separation is employed for spatial diversity.

Fig. 4 depicts the measured ergodic capacity of i.i.d Rayleigh-fading 3×2 MIMO channels with TPD. In this figure $D = 0$, and an angular separation $d\theta$ between contiguous dipoles is employed as a parameter. This situation ($D = 0$, $R = 2$) is not realistic unless a multimode antenna is employed. However, it is useful for comparison purposes. From Fig. 4 it is easily observed that for $d\theta \geq 54^\circ$ the additional increase in terms of MIMO capacity is negligible. A difference of only 5.6% in MIMO capacity was encountered between an angular separation of 54° and that of 90° for a $SNR = 10$ dB. A limitation on performance for both spatial and TPD techniques appears around the same values of the correlation coefficients. Fig. 5 illustrates a comparison between spatial diversity and TPD. Fig. 5 shows how diversity gain depends on wavelength-normalized spatial separation $D = (d/\lambda)$ and angular separation $d\theta(^\circ)$ for 3×2 and 3×3 MIMO systems. It is clearly observed in Fig. 5 that the two techniques perform similarly for increasing the MIMO capacity under the Rayleigh fading environment reproduced in the chambers. As an example, a spatial separation of $\sim 0.14\lambda$ is equivalent to an angular separation of $\sim 36^\circ$.

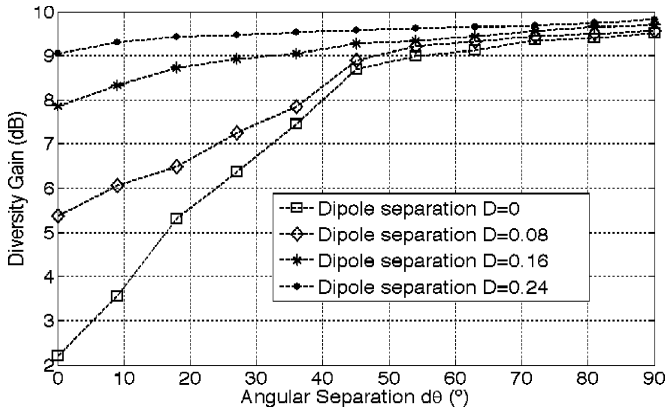

Fig. 6. Measured diversity gain (dB) versus angular separation $\mathrm{d}\theta(^\circ)$ with spatial separation $\mathrm{D} = (\mathrm{d}/\lambda)$ as a parameter for 3×2 MIMO systems.

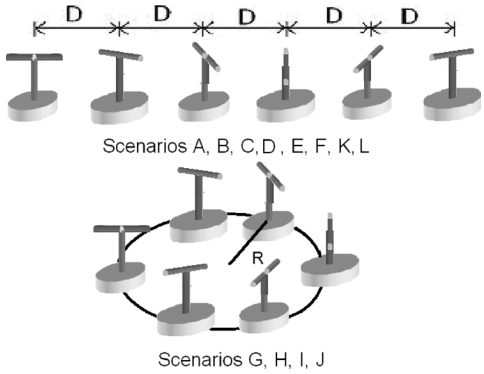

Fig. 7. Geometries of measured receive MIMO array schemes.

IV. Measured Results

A. Measured Combinations

In order to test how a combined spatial-TPD system would perform, Fig. 6 depicts the measured diversity gain for two receiving dipoles separated by both an angular and a spatial separation. Fig. 6 shows how the measured diversity gain depend on angular separation $d\theta(^\circ)$ and wavelength-normalized dipole spatial separation $D = (d/\lambda)$. As expected, the combination of both spatial diversity and TPD provided increased diversity gain with only two elements in the array. The combination has a stronger effect when both separations are not large, i.e., when the spatial separation is large ($D \geq 0.21$), the angular separation can hardly improve the diversity gain, and vice versa when the angular separation is large ($d\theta \geq 45^\circ$), the spatial separation can barely improve the diversity gain. This suggests that a good combination of the two techniques represents the most efficient technique for optimum diversity performance within the same reduced volume made available to the complete array. Results in Fig. 6 also suggest that when the available space for the MIMO array is not limited, the conventional OPD performance cannot be improved with TPD schemes.

In order to evaluate the full potential of TPD techniques for $\mathrm{R} > 2$, combined-diversity systems with both spatial and TPD techniques were tested. Measurements were performed for different linear and circular 3×6 MIMO systems. The diverse scenarios are listed in Table I and illustrated in Fig. 7. It is important to mention here that only one-axis (1D) TPD has been employed, i.e., the dipoles are inclined in one axis only ($\beta_{\max} = 0^\circ$). In this sense, the angular distances in Fig. 7 are assumed as angular displacements in the ZX-plane with respect to Z-axis (vertically) orientated dipoles. No multi-axis (3D) TPD has been tested in this manuscript. Because of the geometrical configuration, for circular arrays the radius $R = r/\lambda$ is also equal to the minimum element spacing $D = d/\lambda$. The correlation coefficients and MIMO capacity performance were measured for the MIMO array formed by the transmitting antennas and the combination of up to 6 receiving dipole antennas. This gives 1 possible 3×6 MIMO system, 6 different 3×5 MIMO systems, 15 different 3×4 MIMO systems, 20 different 3×3 MIMO systems, 15 different 3×2 MIMO systems and 6 different 3×1 MIMO systems. For each MIMO system all angular and spatial separation combinations can be employed, leading to a total of 591 different measured MIMO systems. Yet, not all these systems will provide uniform spatial and angular spacing, and only 312 subsystems are part of the same statistical ensemble. It is interesting to note that more than three receiving antennas were employed in the tested systems of Fig. 7. This combination is simply not possible with conventional OPD.

Yet, a novel hybrid system with three vertically polarized and three horizontally polarized receiving antennas would be possible. With orthogonal polarization alternating between contiguous elements (VHVHVH), the system is really a particular case of TPD with $d\theta = 90^\circ$. In fact, the spatial-only diversity scheme can also be considered a particular case of TPD with $d\theta = 0^\circ$. In addition, another combination with the first three elements oriented in vertical polarization and the last three with horizontal polarization is also used for comparison purposes. This combination can be defined as a purely OPD scheme since it does not corresponds to any particular TPD case.

B. Measured Correlation Coefficients

The measured magnitudes of the complex correlation coefficients for the linear arrays depicted in Fig. 7 are illustrated in Figs. 8 and 9 for small and medium element spacing, respectively. The correlation coefficients depicted in Figs. 8 and 9 for diverse array elements are measured with respect to the first dipole in the array. The results confirmed the enormous potential of TPD for combined-diversity schemes. It is easily observed from Figs. 8 and 9 that the alternating orthogonal polarization scheme (TPD with $d\theta = 90^\circ$) has a jigsaw correlation behavior. In the jigsaw behavior the correlation coefficient between dipole 3 and dipole 1 is higher than the correlation coefficient between dipole 2 and dipole 1. This increase is observed in spite of the fact that the distance between dipole 3 and dipole 1 doubles the distance between dipole 2 and dipole 1. The increase is due to the fact that the third element is co-polarized to the first one, while the second one is cross-polarized to the first one. It is also interesting to observe from Fig. 8 that more general TPD schemes (different from $d\theta = 90^\circ$) depict a different correlation pattern with respect to more conventional OPD. This is expected to have an effect on diversity gain and MIMO capacity.

TABLE I
COMBINED-DIVERSITY MIMO SCHEMES

Antenna separation			Polarization rotation angle						
			TPD	TPD	TPD	TPD	TPD	TPD/OPD	OPD
D(d/λ) R(r/λ)	Array Type	scenario	dθ=0°	dθ=18°	dθ=36°	dθ=54°	dθ=70°	dθ=90° VHVHVH	dθ=90°(x3) VVVHHH
0.000	Linear	A	A1	A2	A3	A4	A5	A6	A7
0.010	Linear	B	B1	B2	B3	B4	B5	B6	B7
0.020	Linear	C	C1	C2	C3	C4	C5	C6	C7
0.025	Linear	D	D1	D2	D3	D4	D5	D6	D7
0.050	Linear	E	E1	E2	E3	E4	E5	E6	E7
0.100	Linear	F	F1	F2	F3	F4	F5	F6	F7
0.010	Circular	G	G1	G2	G3	G4	G5	G6	G7
0.025	Circular	H	H1	H2	H3	H4	H5	H6	H7
0.050	Circular	I	I1	I2	I3	I4	I5	I6	I7
0.100	Circular	J	J1	J2	J3	J4	J5	J6	J7

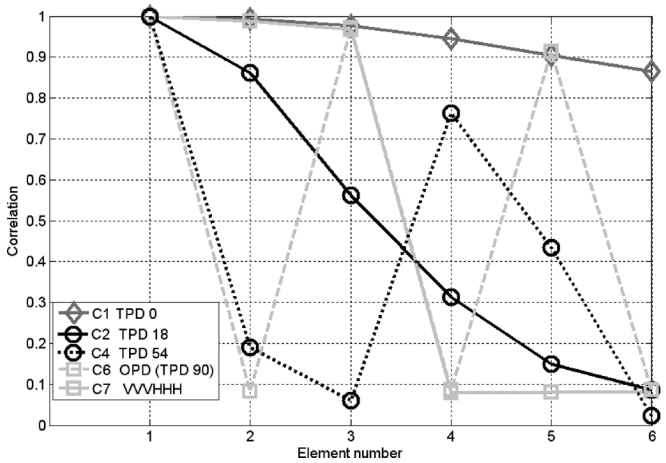

Fig. 8. Measured envelope correlation coefficients with low spatial diversity spacing ($\mathrm{D} = 0.02$).

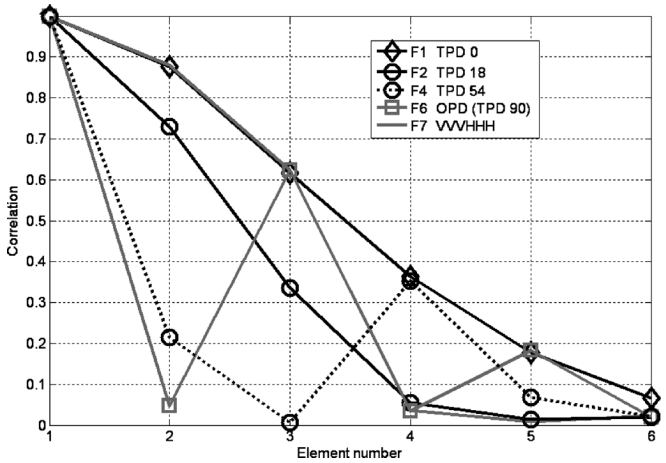

Fig. 9. Measured envelope correlation coefficients with medium spatial diversity spacing ($\mathrm{D} = 0.1$).

C. Measured MIMO Capacity

Fig. 10 depicts the measured MIMO capacities for different combined-diversity systems at $\mathrm{SNR} = 15$ dB. The results in Fig. 10 are extracted only from the 312 systems which were part of the same statistical ensemble. In this figure capacities are depicted for a fixed $\mathrm{SNR} = 15$ dB. Several interesting results are observed from this figure. First, all combined-diversity tested systems provide increased capacity with respect to the spatial-diversity-only linear MIMO system. Secondly, all diverse TPD combinations and conventional OPD perform similarly and close to full capacity (*90%*) when the spatial separation is relatively large, i.e., when the correlation coefficients are small. In addition, when the spatial-diversity antenna spacing D is small enough ($D < 0.07$) to provide correlation coefficients over *0.5*, a considerable capacity reduction is observed for spatial-diversity-only systems in comparison to combined-diversity systems. It is interesting to observe from the previous figure that a combination of spatial and TPD techniques performs at nearly full capacity, even for extremely small spatial antenna spacing ($D = 0.01$). At $\mathrm{SNR} = 15$ dB and for $D < 0.02$, the combination of spatial and TPD techniques nearly doubles the MIMO capacity of the spatial-only linear MIMO system. It is also clear from Fig. 10 that TPD always outperforms conventional OPD diversity for $D < 0.1$. In fact, the pure conventional OPD technique (VVVHHH) shows the worst capacity performance of all tested MIMO systems, except of course the spatial-only one due to the small antenna spacing.

V. DISCUSSION

A. Volume Reduction With TPD

At $\mathrm{SNR} = 15$ dB a MIMO capacity of 12 bits/s/Hz can be achieved with a linear array of a spacing of 0.02λ with a TPD of $d\theta = 54°$ (*Fig. 10*). In contrast, the same capacity performance with conventional orthogonal pure (VVVHHH) or alternating (TPD with $d\theta = 90°$) polarization diversity would require a spacing of 0.055λ or 0.035λ, respectively. A MIMO system with only spatial-diversity techniques would require a spacing over 0.1λ. Consequently, TPD-combined MIMO systems would represent an important volume reduction compared to more conventional techniques. For a quantitative evaluation of volume reduction dipole length, width and inclination has

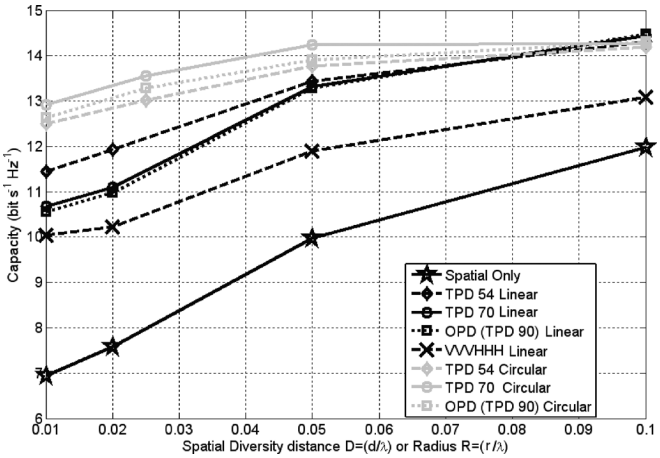

Fig. 10. Measured 3×6 MIMO capacity for diverse scenarios.

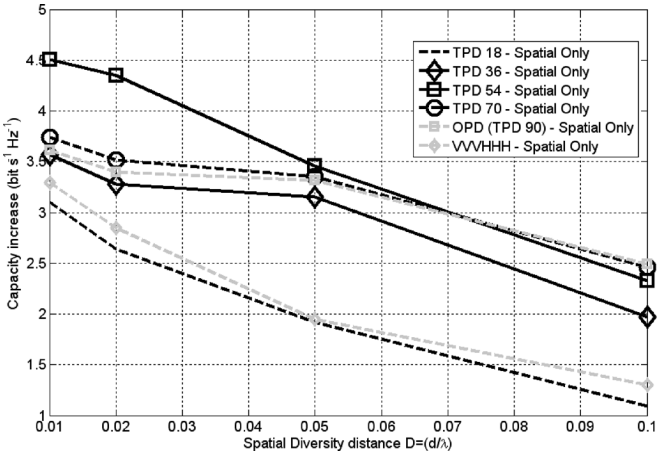

Fig. 11. Measured capacity increment of linear combined-diversity schemes respect to spatial-diversity only.

to be taken into account. Hence, should dipoles be used as receiving antennas TPD-combined MIMO systems can provide a volume reduction of 82% and 72% with respect to conventional pure and alternating OPD techniques, respectively. In this sense, it is clear that TPD techniques provide a considerable volume reduction respect to conventional OPD techniques for the same final measured capacity. It has to be mentioned, however, that for realistic use the provided volume reduction figures would have to be modified to account for each specific antenna-occupied volume in order to get the desired polarization state. Nevertheless, specific and different $d\theta$ values are required in TPD to outperform conventional pure or alternating OPD techniques. This requires a specific analysis.

B. Comparison Between TPD and OPD

TPD has been found to perform well for small element spacing when combined to spatial diversity. Thus, a comparison between spatial-combined systems using either TPD or conventional OPD was performed. In Figs. 11 and 12 the measured capacity increase with respect to the spatial-only diversity scheme (equivalent to TPD with $d\theta = 0°$) for $\mathrm{SNR} = 15$ dB is depicted for linear and circular arrays, respectively. From these figures it is clear again that TPD outperforms conventional OPD for small element spacing ($D < 0.07$). Yet, as the spatial diversity spacing increases, the extra multiplexing gain obtained by either TPD or conventional OPD vanishes [11]. Consequently the difference between TPD and conventional OPD performance decreases, as expected.

This agrees well with early reported results for combined diversity schemes [11]. This indicates that while the benefits of polarization diversity are additive, there is a saturation effect. It is interesting to observe from Fig. 11 that the TPD scheme with $d\theta = 54°$ outperforms any other combination for all tested radii, including conventional alternating OPD schemes (TPD with $d\theta = 90°$). This suggests that the saturation effect of combining TPD to spatial-only diversity systems is related to small volumes rather than simply small element spacing. Measured results show that TPD outperforms conventional OPD for array radius of up to 0.1λ. This is equivalent to an array available spheroid volume of $4.19 \times 10^{-3}\lambda^3$ (or a cube with a 5.4 cm side), larger than any handset volume made currently available

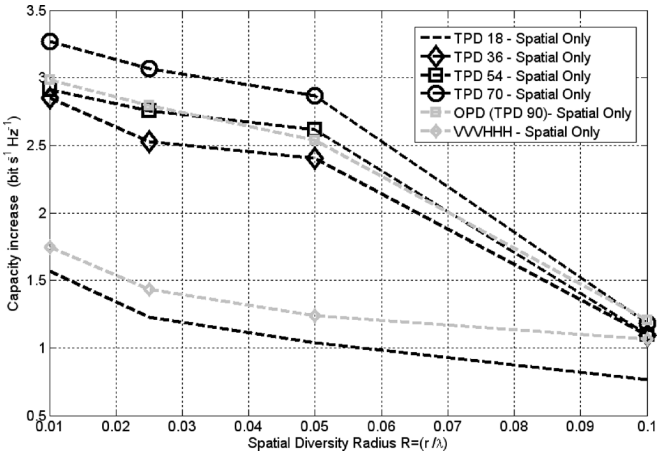

Fig. 12. Measured capacity increment of circular combined-diversity schemes respect to spatial-diversity only.

to the antenna designer. Consequently, it is clear that TPD outperforms conventional OPD for handset MIMO when more than two antennas are employed in reception. This is reported here for the first time.

With only two receiving antennas conventional OPD performs better than any other scheme. Consequently, two-branch $\pm 45°$ polarization diversity substituted spatial-diversity in commercial GSM base station antenna arrays. With three or more antennas, however, results have shown that for limited volumes TPD performs better. This is attributed to the fact that when the antennas are close to each other, the MIMO performance is not only based on the correlation between the first and second antenna, which is low due to the orthogonality, but also on the correlation between the first and the third or the second and the fourth, and so on. With the proposed TPD schemes and OPD schemes for more than two antennas, the correlation between all elements has to be considered. With the OPD scheme the correlation between the first and third and second and fourth is high as they have the same polarization state. Optimum $d\theta$ values for TPD were found by simulations and measurements. With the proposed TPD rotation there is no orthogonality between the first and second element, thus with higher correlation

between these two elements than in the orthogonal scheme. Yet, TPD also provides for different polarization states between the first and third antennas or second and fourth antennas. This reduces the correlation between these pairs in contrast to what happens for OPD, accounting for the better final performance of TPD. Despite its simplicity and generality, TPD cannot be found in the literature, except of course our previous short letter [11]. OPD can really be considered a particular case of TPD with $d\theta = 90°$.

C. TPD Performance in Non-Isotropic Scenarios

In order to provide more general results that will help a designer use the TPD concept effectively, more measurements were performed for non-isotropic environments using the MIMO Analyzer. Both diversity gain and capacity performance of TPD under the typical isotropic environment (Scenario E with $\mathrm{AS} = 82°$ and $\mathrm{MPC} = 24$) were compared to those obtained with two different non-isotropic environments. In Scenario K four PTFE 30 cm high hollow cylinders of 5 cm radius filled with lossy CENELEC Head Simulating Liquid (HSL) at the frequency of interest are introduced in the empty chamber. The filled-cylinders make the Q-factor of the chamber decrease, slightly increasing the K-factor, with a final $\mathrm{AS} = 45°$ and $\mathrm{MPC} = 12$. In Scenario L two absorbers are used within the chamber. Scenario L reduces the number of resolvable multipath components (MPC) by absorbing specific directions, providing a final $\mathrm{AS} = 36°$ and $\mathrm{MPC} = 15$.

It is expected that the larger the angular spread, the better potential performance for multi-polarized MIMO arrays. This is because of the combined effect of several waves arriving from different directions, which may increase the number of independent channels. This may in turn result in a possible incoherent summation of all these different channels, should they be captured by the different antenna elements. These degrees of freedom may be attributed to a combination of different polarizations and patterns. In this sense OPD is expected to require more AS than TPD for energy to be decoupled into orthogonal polarization states rather than to closer polarization states. As expected, both diversity gain and capacity performance were higher in all cases (TPD and OPD) for the emulated isotropic environment. Figs. 13 and 14 depict the measured diversity gain loss and capacity loss respect to the ideal uncorrelated 3×6 Rayleigh, respectively. In Fig. 13 it is observed that there is always a TPD combination outperforming OPD. Likewise, from Fig. 14 it is again observed that there is always a TPD combination with less capacity loss than OPD. It is yet important to also note that the outperforming gain of TPD respect to OPD for reduced volumes shrinks with decreasing AS. This agrees well with the fact that a suitable level of scattering has to be made available to gain sufficient depolarization from a single polarization source [39].

D. Possible Distortion of Multi-Polarization Performance

While the elevation angular spread emulated in the chambers may encounter some differences to that of LoS, indoor and in-vehicle scenarios, it is a good approximation for outdoor environments in the absence of LoS [20], [21]. A significant elevation angular spread, however, is known to have a positive effect on final

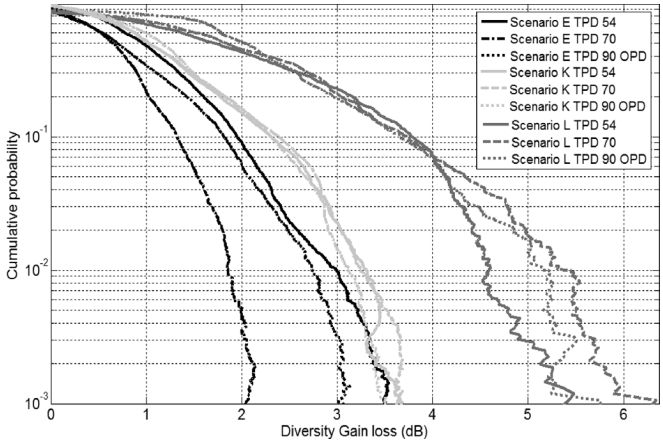

Fig. 13. Diversity gain loss with respect to the ideal uncorrelated 3×6 Rayleigh.

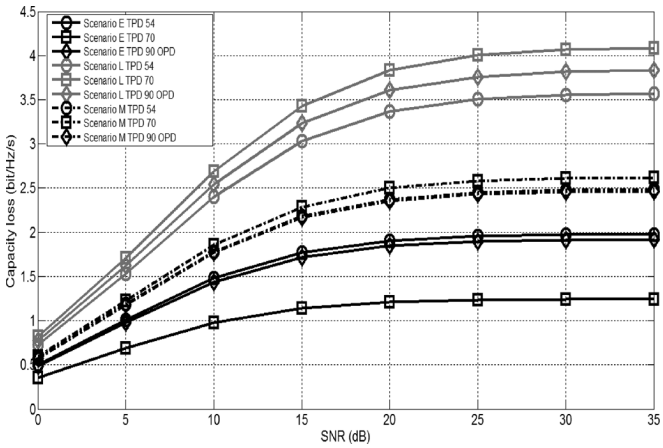

Fig. 14. Capacity loss with respect to the ideal uncorrelated 3×6 Rayleigh.

performance when OPD is considered, and this may also have an effect on TPD. Similarly, for reduced volumes the effect of mutual coupling will certainly have an effect on both TPD and OPD performance. Likewise, the effect of the presence of the user will alter the radiation efficiency of the MIMO array elements, and it will do so in a different way for each element. Finally, the balanced polarization response of the chambers and the employed normalization could artificially favor polarization diversity schemes in comparison to existing typical environments with a vertically polarized transmitter. These systems produce higher power at the receiver in the vertical polarization than in any other state. Thus, the performance of TPD may also be distorted when using existing transmitting diversity schemes which have not been thought for TPD at the handset. Consequently, all these realistic effects require future research for accurate prediction of TPD optimum angular spacing in handset MIMO.

VI. Conclusion

While spatial diversity has already been identified in the literature as an excellent candidate for improving diversity gain and MIMO capacity for wireless systems, results presented in this paper demonstrate that true polarization diversity (TPD) is equally important and particularly significant when combined

to spatial-diversity schemes. Not only TPD has been made equivalent to spatial diversity, but is also particularly suitable for improving current diversity gain and MIMO capacity of spatial-only diversity systems with volume-limited sizes. Simulated and measured results in over 591 different MIMO systems have shown that TPD outperforms conventional orthogonal polarization diversity (OPD) for reduced volumes. In addition, TPD can be effectively combined with spatial diversity to nearly double MIMO capacity for the same available volume. This performance of TPD is not invariant with spatial distance D. If there is no limitation in volume and D is large enough, alternating OPD will outperform TPD. The recently proposed handset MIMO for 4G systems, however, imposes volume restrictions that make TPD perform better than OPD. Consequently, TPD could be useful in handset MIMO or for small MIMO arrays, for which 80% volume reductions have been demonstrated. The same combined-system performance with spatial-only diversity schemes would require unaffordable additional volume. TPD performance results obtained in both isotropic and non-isotropic environments allow for determining the fundamental behavior of this technique. The technique is patent protected by EMITE Ing. Research is envisaged for Rician-like or more general Nagakami-m distribution fading environments and TPD with multi-axis inclination angles (3D TPD).

REFERENCES

[1] M. Kang and M.-S. Alouni, "Capacity of correlated MIMO Rayleigh channels," *IEEE Trans. Wireless Commun.*, vol. 5, pp. 143–155, Jan. 2006.

[2] M. Kang and M.-S. Alouni, "Capacity of correlated MIMO Rician channels," *IEEE Trans. Wireless Commun.*, vol. 5, pp. 112–120, Jan. 2006.

[3] T. Svantesson, "Correlation and channel capacity of MIMO systems employing multimode antennas," *IEEE Trans. Veh. Technol.*, vol. 51, pp. 1304–1312, Nov. 2002.

[4] A. Goldsmith, S. A. Jafar, N. Jindal, and S. Vishwanath, "Capacity limits of MIMO channels," *IEEE J. Sel. Areas Commun.*, vol. 21, pp. 684–702, Jun. 2003.

[5] V. Erceg, H. Sampath, and S. Catreux-Erceg, "Dual- polarization versus single-polarization MIMO channel measurement results and modeling," *IEEE Trans. Wireless Commun.*, vol. 5, pp. 28–33, Jan. 2006.

[6] W. C. Y. Lee, "Effects of correlation between two mobile radio base station antennas," *IEEE Trans. Commun.*, vol. 21, pp. 1214–1224, Nov. 1973.

[7] F. Adachi, M. T. Feeney, A. G. Williamson, and J. D. Parsons, "Cross-correlation between the envelopes of 900 MHz signals received at a mobile radio base station site," *Proc. Inst. Elect. Eng. Part F. Commun., Radar Signal Process.*, vol. 133, no. 6, pp. 506–5 11, Oct. 1986.

[8] R. G. Vaughan, "Polarization diversity in mobile communications," *IEEE Trans. Veh. Technol.*, vol. 39, pp. 177–186, Aug. 1990.

[9] M. C. Tumbuka and D. J. Edwards, "Investigation of tri-polarised MIMO technique," *Electron. Lett.*, vol. 41, no. 3, pp. 137–138, Feb. 2005.

[10] N. K. Das, T. Inoue, T. Taniguchi, and Y. Karasawa, "An experiment on MIMO system having three orthogonal polarization diversity branches in multipath-rich environment," in *Proc. IEEE 60th Veh. Technol. Conf.*, Sep. 2004, vol. 2, pp. 1528–1532.

[11] J. F. Valenzuela-Valdés, M. A. García-Fernández, A. M. Martínez-González, and D. A. Sánchez-Hernández, "The role of polarization diversity for MIMO systems under Rayleigh-fading scenarios," *IEEE Antennas Wireless Propag. Lett.*, vol. 5, pp. 534–536, 2006.

[12] C. Oestges, V. Erceg, and A. J. Paulraj, "Propagation modeling for MIMO multipolarized fixed wireless channels," *IEEE Trans. Veh. Technol.*, vol. 53, pp. 644–654, May 2004.

[13] J. F. Valenzuela-Valdés, A. M. Martínez-González, and D. Sánchez-Hernández, "Estimating combined correlation functions for dipoles in Rayleigh-fading scenarios," *IEEE Antennas Wireless Propag. Lett.*, vol. 6, pp. 349–352, 2007.

[14] D. Gesbert, M. Shafi, D.-S. Shiu, P. J. Smith, and A. Naguib, "From theory to practice: An overview of MIMO space-time coded wireless systems," *IEEE J. Sel. Areas Commun.*, vol. 21, pp. 281–302, Apr. 2003.

[15] G. Foschini and M. Gans, "On limits of wireless communication in a fading environment when using multiple antennas," *Wireless Personal Commun.*, pp. 311–335, Mar. 1998.

[16] E. Telatar, "Capacity of multi-antenna Gaussian channels," *Eur. Trans. TeleCommun.*, vol. 10, no. 6, pp. 585–595, Nov./Dec. 1999.

[17] H. Shin and J. H. Lee, "Capacity of multiple-antenna fading channels: Spatial fading correlation, double scattering, and keyhole," *IEEE Trans. Inf. Theory*, vol. 49, pp. 2636–2647, Oct. 2003.

[18] A. F. Molish, M. Z. Win, Y.-S. Choi, and J. H. Winters, "Capacity of MIMO systems with antenna selection," *IEEE Trans. Wireless Commun.*, vol. 4, pp. 1759–1772, Jul. 2005.

[19] K. Rosengren and P. S. Kildal, "Study of distributions of modes and plane waves in reverberation chamber for characterizacion of antennas in multipath environment," *Microw. Opt. Technol. Lett.*, vol. 30, pp. 386–391, 2001.

[20] M. Shafi, M. Zhang, A. L. Moustakas, P. J. Smith, A. F. Molisch, F. Tufvesson, and S. H. Simon, "Polarized MIMO channels in 3-D: Models, measurements and mutual information," *IEEE J. Sel. Areas Commun.*, vol. 24, pp. 514–527, Mar. 2006.

[21] T. Neubauer and P. C. F. Eggers, "Simultaneous characterization of polarization matrix components in pico cells," in *Proc. IEEE Veh. Technol. Conf.*, 1999, pp. 1361–1365.

[22] P. S. Kildal, K. Rosengren, J. Byun, and J. Lee, "Definition of effective diversity gain and how to measure it in a reverberation chamber," *Microw. Opt. Technol. Lett.*, vol. 34, no. 1, pp. 56–59, Jul. 2002.

[23] P. S. Kildal and K. Rosengren, "Correlation and capacity of MIMO systems and mutual coupling, radiation efficiency, and diversity gain of their antennas: Simulations and measurement in a reverberation chamber," *IEEE Commun. Mag.*, pp. 104–112, Dec. 2004.

[24] J. F. Valenzuela-Valdés, A. M. Martínez-González, and D. A. Sánchez-Hernández, "Emulation of MIMO non-isotropic fading environments with reverberation chambers," *IEEE Antennas Wireless Propag. Lett.*, vol. 7, pp. 325–328, 2008.

[25] C. L. Holloway, D. A. Hill, J. M. Ladbury, P. F. Wilson, G. Koepke, and J. Coder, "On the use of reverberation chambers to simulate a Rician radio environment for the testing of wireless devices," *IEEE Trans. Antennas Propag.*, vol. 54, pp. 3167–3177, 2006.

[26] O. Delangre, P. D. Doncker, M. Lienard, and P. Degauque, "Wideband analysis of coupled reverberation chambers for testing MIMO systems," presented at the IEEE Int. Symp. on Personal, Indoor and Mobile Radio Commun. (PIMRC), Sep. 2006.

[27] O. Delangre, S. Van Roy, P. De Doncker, M. Lienard, and P. Degauque, "Modeling in-vehicle wideband wireless channels using reverberation chamber theory," in *Proc. IEEE Veh. Technol. Conf.*, Sep. 2007, pp. 2149–2153.

[28] O. Delangre, P. De Doncker, M. Lienard, and P. Degauque, "Propagation channel modelling in coupled reverberation chambers for testing MIMO systems," presented at the COST 273 TD(05) 85, Jun. 2005.

[29] Z. Yun and M. F. Iskander, "MIMO capacity for realistic wireless communications environments," in *Proc. IEEE Antennas Propag. Society Int. Symp.*, Jun. 2004, pp. 1231–1234.

[30] P. Corona, G. Ferrara, and M. Migliaccio, "Reverberating chamber electromagnetic field in presence of an unstirred component," *IEEE Trans. Electromagn. Compat.*, vol. 42, pp. 111–115, 2000.

[31] T. S. Rappaport, *Wireless Commun.: Principles and Practice*. Upper Saddle River, NJ: Prentice-Hall, 1996.

[32] P. S. Kildal, C. Carlsson, and J. Yang, "Measurement of free space impedances of small antennas in reverberation chambers," *Microw. Opt. Technol. Lett.*, vol. 32, pp. 112–115, 2002.

[33] P. S. Kildal *et al.*, "Radiation efficiency, correlation, diversity gain and capacity of a six-monopole antenna array for a MIMO system: Theory, simulation and measurement in reverberation chamber," *Proc. Inst. Elect. Eng. Microw. Antennas Propag.*, vol. 152, no. 1, pp. 7–16, Feb. 2005.

[34] K. Rosengren, P. S. Kildal, C. Carlsson, and J. Carlsson, "Characterization of antennas for mobile and wireless terminals in reverberation chambers: Improved accuracy by platform stirring," *Microw. Opt. Technol. Lett.*, vol. 30, pp. 391–397, 2001.

[35] P. S. Kildal and C. Carlsson, "Detection of a polarization imbalance in reverberation chambers and how to remove it by polarization stirring when measuring antenna efficiencies," *Microw. Opt. Technol. Lett.*, vol. 34, no. 2, pp. 145–149, Jul. 2002.

[36] M. A. Jensen and J. W. Wallace, "A review of antennas and propagation for MIMO wireless communications," *IEEE Trans. Antennas Propag.*, vol. 52, pp. 2810–2824, Nov. 2004.
[37] P. S. Kildal and C. Carlsson, "Study of polarization stirring in reverberation chambers used for measuring antenna efficiencies," in *Proc. IEEE Antennas Propag. Society Int. Symp.*, 2002, vol. 2, pp. 486–489.
[38] S. Kozono, T. Tsuruhara, and M. Sakamoto, "Base station polarization diversity reception for mobile radio," *IEEE Trans. Veh. Technol.*, vol. 33, pp. 301–306, Nov. 1984.
[39] T. W. C. Brown, S. R. Saunders, S. Stavrou, and M. Fiacco, "Characterization of polarization diversity at the mobile," *IEEE Trans. Veh. Technol.*, vol. 56, pp. 2440–2447, Sep. 2007.

Juan F. Valenzuela-Valdés was born in Marbella, Spain. He received the Degree in Telecommunications Engineering from the Universidad de Malaga, Spain, in 2003 and the Ph.D. degree from the Universidad Politécnica de Cartagena, Spain, in May 2008.

In 2004 he worked at CETECOM (Malaga). In 2004, he joined the Department of Information Technologies and Communications, Universidad Politécnica de Cartagena, Spain. In 2007 he joined EMITE Ing, Spain, as Head of Research. His current research areas cover MIMO communications, multimode-stirred chambers and SAR measurements.

Miguel A. García-Fernández was born in Cartagena, Spain. He received the Degree in Telecommunications Engineering from the Universidad Politécnica de Cartagena, Spain, in 2005.

In 2005, he joined the Department of Information Technologies and Communications, Universidad Politécnica de Cartagena, Spain, where he is currently working toward the Ph.D. degree. His current research areas cover SAR measurements and thermoregulatory processes due to electromagnetic field exposure.

Antonio M. Martínez-González received the Dipl.-Ing. degree in Telecommunications Engineering from the Universidad Politécnica de Valencia, Spain, in 1998 and the Ph.D. degree from the Universidad Politécnica de Cartagena, Spain, in early 2004.

From 1998 to September 1999, he was employed as a Technical Engineer at the Electromagnetic Compatibility Laboratory, Universidad Politécnica de Valencia, where he developed assessment activities and compliance certifications with European directives related with immunity and emissions to electromagnetic radiation from diverse electrical, electronic and telecommunication equipment. Since September 1999, he has been an Assistant lecturer at the Universidad Politécnica de Cartagena. His research interest is focused on electromagnetic dosimetry and radioelectric emissions.

Dr. Martínez-González was awarded with the Spanish National Prize from Foundation Airtel and Colegio Oficial de Ingenieros de Telecomunicación de España for the Best Final Project on Mobile Communications in 1999.

David A. Sánchez-Hernández (M'00–SM'06) received the Dipl.-Ing. degree in Telecommunications engineering from the Universidad Politécnica de Valencia, Spain, in 1992 and the Ph.D. degree from King's College, University of London, London, U.K., in early 1996.

From 1992 to 1994, he was employed as a Research Associate for The British Council-CAM at King's College London where he worked on active and dual-band microstrip patch antennas. In 1994, he was appointed EU Research Fellow at King's College London, working on several joint projects at 18, 38 and 60 GHz related to printed and integrated antennas on GaAs, microstrip antenna arrays, sectorization and diversity. In 1997, he returned to the Universidad Politécnica de Valencia, Spain, where was co-leader of the Antennas, Microwaves and Radar Research Group and the Microwave Heating Group. In early 1999, he received the Readership from Universidad Politécnica de Cartagena, and was appointed Vice Dean of the School for Telecommunications Engineering and leader of the Microwave, Radiocommunications and Electromagnetism Engineering Research Group. In late 1999, he was appointed Vice Chancellor for Innovation and Technology Transfer at Universidad Politécnica de Cartagena and became a member of several foundations and societies for the promotion of R&D in the Autonomous Region of Murcia, in Spain. In May 2001, he was appointed official advisor in technology transfer and member of The Industrial Advisory Council of the Autonomous Government of the Region of Murcia, in Spain, and in May 2003 he was appointed Head of Department. He has published over 40 scientific papers and over 80 conference contributions, and is a reviewer of several international journals. He holds five patents. His current research interests encompass all aspects of the design and application of printed multi-band antennas for mobile communications, electromagnetic dosimetry issues and MIMO techniques for wireless communications.

Dr. Sánchez-Hernández is a Chartered Engineer (CEng), Institution of Engineering and Technology (IET) Fellow, Ampere Board member, CENELEC TC106X member, and is the recipient of the R&D J. Langham Thompson Premium, awarded by the IET, as well as other national and international awards.